

Comparison of CdS nano films deposited by thermal evaporation and spray pyrolysis techniques

A. N. Abouelkhir^{a,*}, E. R. Shaaban^{b,c}, M. Tag El-Dine^a, K. I. Hussain^d, I. S. Yahia^e

^aPhysics Department, Faculty of Science, New Valley University, Egypt

^bPhysics Department, Faculty of Science, Islamic University of Madinah, Almadinah Al-Munawarah 42351, Saudi Arabia

^cDepartment of Physics, Faculty of Science, Al-Azhar University, Assiut 71542, Egypt

^dDepartment of Radiological Sciences, College of Applied Medical Sciences, King Khalid University, Abha 61421, Saudi Arabia

^eLaboratory for environmental and biomedical applications (NLEBA), Semiconductor Lab., Physics Department, Faculty of Education, Ain Shams University, Roxy, Cairo

Cadmium sulfide was prepared by first turning it into a powder, which was then used to evaporate heat to create thin films. Additionally, the spray pyrolysis method was used to produce films of cadmium sulfide. A structural comparison using the crystallize size and lattice parameters. Furthermore for the prepared samples, an analysis of their optical characteristics was conducted through measurements of absorbance, transmission, and reflection, resulting in the determination of the energy gap.

(Received December 9, 2023; Accepted February 8, 2024)

Keywords: Cadmium sulfide, Nanoparticles, Thermal evaporation technique, Spray pyrolysis technique, Optical and structural study

1. Introduction

Cadmium sulfide (CdS) is a type II-VI semiconductor that displays intrinsic n-type conductivity resulting from sulfur vacancies caused by an excess of cadmium atoms. [1]. At a temperature of 300K, bulk CdS possesses a band gap energy of 2.42 eV and exhibits absorption maxima at 515nm. [2]. Cadmium sulfide can adopt three distinct crystal structures: wurtzite, zinc blend, and high-pressure rock-salt phase. Due to its remarkable stability, exceptional physical, chemical, and structural properties, widespread availability, and ease of preparation and handling, CdS has numerous potential applications across a variety of fields. –As a result of quantum size effects and surface effects, CdS can exhibit novel properties in the areas of optics, electronics, magnetism, chemistry, and structure, which could have significant technological implications. [3].

Different techniques have been successfully employed to prepare CdS NPs and CdS thin films such as spray pyrolysis [4], thermal evaporation [5], chemical vapor deposition and electrodeposition [6]. The current work aims to investigate the structural and optical characteristics of CdS thin films deposited via spray pyrolysis and thermal evaporation.

2. Experimental details

2.1. Synthesize the CdS nanoparticles

To synthesize the CdS nanostructures, Sigma-Aldrich Pvt. Ltd. was the source of cadmium chloride ($\text{CdCl}_2 \cdot \text{H}_2\text{O}$), sodium sulfide (Na_2S), and Cetyltrimethylammonium bromide (CTAB). To synthesize pure CdS nanostructures, a microwave-assisted approach was utilized. Initially, 0.5M

*Corresponding author: aboelkhier@hotmail.com
<https://doi.org/10.15251/CL.2024.212.161>

cadmium chloride ($\text{CdCl}_2 \cdot \text{H}_2\text{O}$) was mixed with 50 mL of double-distilled water (DDW) in a cleaned beaker and stirred for 10 minutes at 70 °C to form solution A. Next, 0.5 g of Cetyltrimethylammonium bromide (CTAB) was added to solution A while continuously stirring for 30 minutes. Meanwhile, another beaker containing 50 mL of DDW was used to prepare a solution of 0.5M sodium sulfide, referred to as solution B. Each B solution was slowly added to the respective A solution with regular stirring. The formation of CdS nanostructures was indicated by the appearance of a yellow precipitate within a few seconds. The resulting solution was transferred to cylindrical flasks and subjected to microwave treatment at 700W power for 15 minutes, followed by cooling at ambient temperature. The treated solution was washed several times using DDW, and the resulting powders were collected and annealed at 100 °C.

2.2. Synthesis thin films by spray pyrolysis method

To fabricate a CdS film on a glass substrate, analytical grade Cadmium chloride (CdCl_2) and Thiourea ($\text{CS}(\text{NH}_2)_2$) were used. The glass substrate was systematically cleaned before depositing the films. To prepare the solution, CdCl_2 and Thiourea were mixed in 10 ml of solvent. The films were obtained by spray deposition of the solution onto the substrate while keeping the substrate at 300 °C. During the spray process, the spacing between the nozzle and the glass was maintained at 50 mm and the gas flow rate was set to 1 Kg/m². Once the deposition process was completed, the chamber was allowed to cool down naturally.

2.3. Synthesize thin films by vacuum evaporation method

CdS powders were pressed to form circular disk-shaped pellets, which were used as starting materials for depositing thin films on clean glass substrates. The thin films were deposited on the glass substrates using the electron beam evaporation method in a coating unit type Edward 306 Auto under high vacuum conditions at room temperature. The glass substrates were carefully cleaned using an ultrasonic hot bath, distilled water, and pure alcohol prior to the deposition process. The compressed disks of CdS powder were inserted into a graphite boat, and the vacuum system was left for a period of time to reach an operating pressure of approximately 9×10^{-7} mbar. To ensure good homogeneity of the film thickness, the glass substrates were rotated using a motor attached to the coating unit at a low speed of 2 rpm.

3. Result and discussion

3.1. Chemical Composition

3.1.1. Energy dispersive X-ray (EDX) spectroscopy

Figure (1) displays the typical EDX spectra of prepared CdS samples. The EDX spectrum of pure CdS samples confirms the chemical purity of the samples, with strong peaks related to Cd and S being obtained.

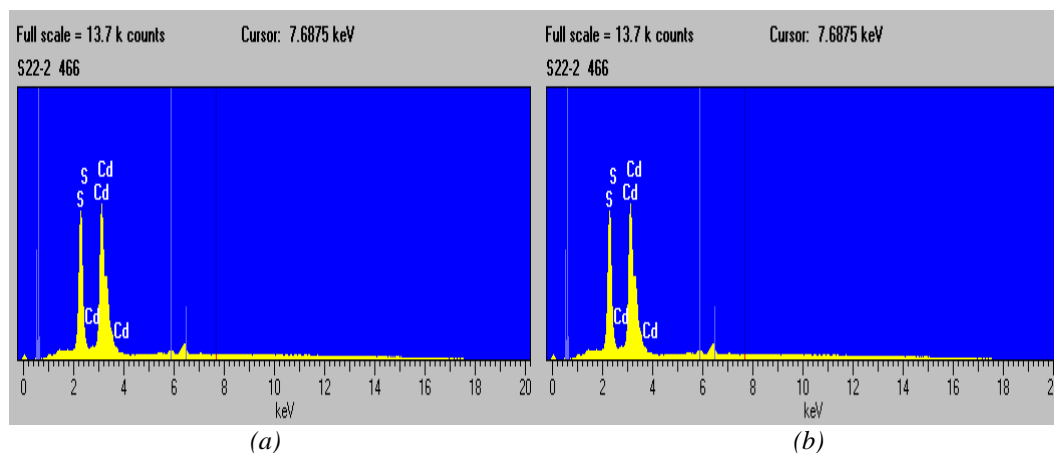


Fig.1. EDX spectra of: a) CdS NP., b) CdS film prepared by spray pyrolysis technique.

3.2. Structural characterization

CdS NP was prepared and annealed at temperature 100°C. The annealing process at 100°C resulted in the formation of a cubic phase, as indicated by the prominent peaks observed at 26.45°, 43.88°, and 51.97°, corresponding to the (111), (220), and (311) crystallographic planes, respectively (Figure 2a).

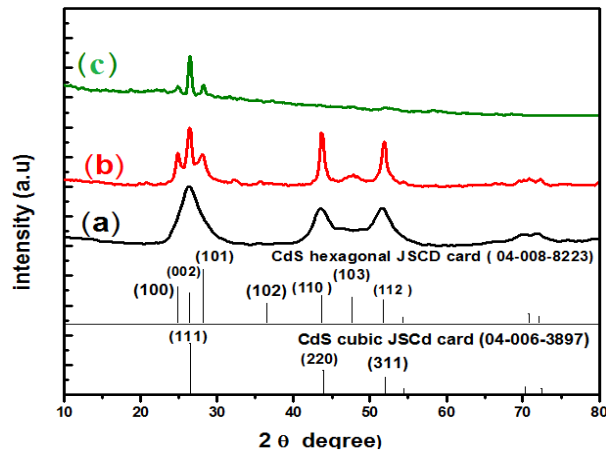


Fig. 2. X-ray diffraction spectra of prepared samples: a) as prepared CdS nano powder, b) CdS prepared by spray pyrolysis technique, c) Thermal evaporated CdS thin film.

Upon increasing the temperature to 300°C in spray pyrolysis technique, the angular region between 20° and 30° exhibited a transition from a single peak to a three-peak pattern (Figure 2b). This change signifies the emergence of (100) and (101) peaks, indicating a shift in the crystalline structure from cubic, zinc blende structure to a hexagonal wurtzite structure. Banerjee et al. [7] have previously reported that the hexagonal phase can exist in both bulk and monocrystalline CdS, while the cubic phase is only observed in nanocrystalline CdS. The primary distinction between the hexagonal and cubic phases lies in their stacking sequences and symmetry, although both structures possess the same coordination number. Specifically, the hexagonal phase exhibits an ABCABCABC stacking sequence, while the cubic structure follows an ABABAB stacking sequence. Notably, there is existing literature discussing the phase transformation dependent on particle size [8].

Also, thermal evaporated CdS sample was indexed as having a hexagonal phase according to JSCD card as shown in Figure (2c).

The crystallite size of the samples was calculated using the Scherrer equation [9] based on diffraction peaks.

$$D = \frac{0.9\lambda}{\beta \cos\theta} \quad (1)$$

The particle size of the prepared CdS samples was determined to be 4.2 nm, 10.4 nm and 27.3 nm for (a), (b), and (c) samples using the Scherrer equation, which takes into account the Bragg diffraction angle (θ), the X-ray wavelength (λ), and the full width at half maximum (FWHM) of the peak (β).

For CdS thermal evaporated sample, FWHM decrease, indicating increased in the crystalline nature of the samples.

Table 1 presents the determined structural parameters of three prepared CdS samples.

The lattice parameter 'a' of cubic zinc blende structure is calculated for the prepared NPs by using Bragg's law [6]:

$$2d_{hkl}\sin\theta = n\lambda \quad (2)$$

where ‘ θ ’ is the peak position, ‘ λ ’ is the wave length of X rays, ‘ n ’ is the order of diffraction usually ($n = 1$) and ‘ d_{hkl} ’ is the inter planer separation corresponding to Miller indices ‘ hkl ’ which defined by the following equations [6,11]:

$$\frac{1}{d_{hkl}^2} = \frac{h^2 + k^2 + l^2}{a^2} \quad (3)$$

$$a = \frac{\lambda}{2 \sin \theta} \sqrt{h^2 + k^2 + l^2} \quad (4)$$

$$v = a^3 \quad (5)$$

where ‘ v ’ is the unit cell volume of the cubic zinc blende structure.

Table 1. First 2θ position, the lattice parameter, interplanar spacing and cell volume of CdS samples.

Code	Samples	‘ 2θ ’ Deg. (111)	Particle size (nm)	‘d’ Spacing (nm)	‘a’ Lattice Parameter (nm)	‘ v ’ Cell volume (nm) ³
S1	As prepared NP.	26.34	4.2	0.3386	0.586	0.2012
S2	Spray pyrolysis	26.43	10.4	0.3369	0.583	0.1981
S3	Thermal evaporation	26.51	27.3	0.3359	0.581	0.1961

The lattice parameters for hexagonal phase were estimated by using the Bragg’s law then, the inter-planner spacing is defined as [11]:

$$\frac{1}{d_{hkl}^2} = \frac{4}{3} \left(h^2 + hk + \frac{l^2}{c^2} \right) \quad (6)$$

$$v = \frac{\sqrt{3}}{2} a^2 c = 0.866 a^2 c \quad (7)$$

where ‘ hkl ’ are the miller indices of the crystallographic planes, ‘ a ’ & ‘ c ’ are the lattice parameters, ‘ v ’ is Cell volume of the hexagonal structures. The calculated data are reported in the Table (2).

Table 2. Estimating values of lattice parameter, cell volume and particle size for CdS samples.

CdS preparation technique	Lattice parameter (nm)		Cell volume (v) nm ³	Structure
	a	c		
As prepared NP.	0.595		0.1931	cubic
Spray pyrolysis	0.451	0.643	0.110	hexagonal
Thermal evaporation	0.472	0.667	0.123	hexagonal

3.3. Optical Properties

Figure 3 illustrates the absorption spectra of the samples in the ultraviolet-visible (UV-vis) light range. The absorption edge observed around wavelength value 510 nm corresponds to the characteristic absorption band edge of CdS NPs. This edge is shifted towards the blue end of the spectrum compared to the bulk band gap of CdS (512 nm) due to the quantum confinement effect.

However, in the case of CdS thermal evaporated thin film sample the absorption edge is slightly shifted towards shorter wavelengths, resulting in a blue shift compared to CdS nanopowder.

The optical absorption coefficient (α) was determined using the Beer-Lambert law, which relates the absorbance (A) of a sample to its thickness (T) and the measured spectral data:

$$\alpha = 2.303 A/T \quad (8)$$

In order to calculate the optical band gap of the nanoparticles (NPs), Tauc's relation was employed [8]:

$$(\alpha h\nu)^{1/n} = (h\nu - E_g) \quad (9)$$

Here, $h\nu$ represents the photon energy, E_g is the optical band gap of the NPs, α is the absorption coefficient, A is a constant, and the exponent n depends on the type of transition. For allowed direct and indirect band gaps, n is equal to 1/2 and 2, respectively.

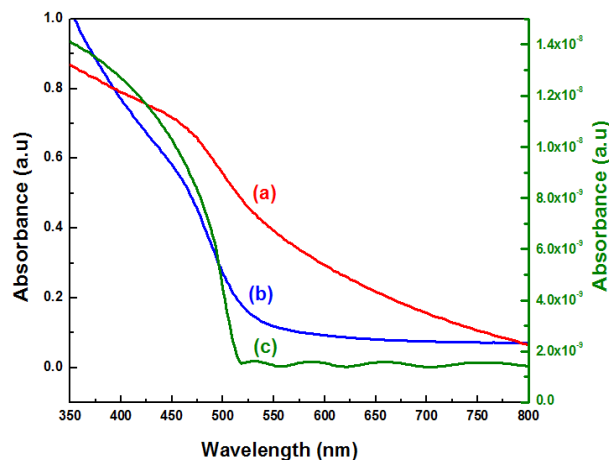


Fig. 3. Optical absorbance of: a) as prepared CdS nanopowder, b) CdS prepared by spray pyrolysis technique c) thermal evaporated CdS thin film.

Figure (4) depicts a plot of $(\alpha h\nu)^2$ versus photon energy ($h\nu$), which was found to be linear at the absorption edge, indicating a direct transition. The energy band gap was determined by extrapolating the straight-line portion to the energy axis at $(\alpha h\nu)^2$ equal to zero.

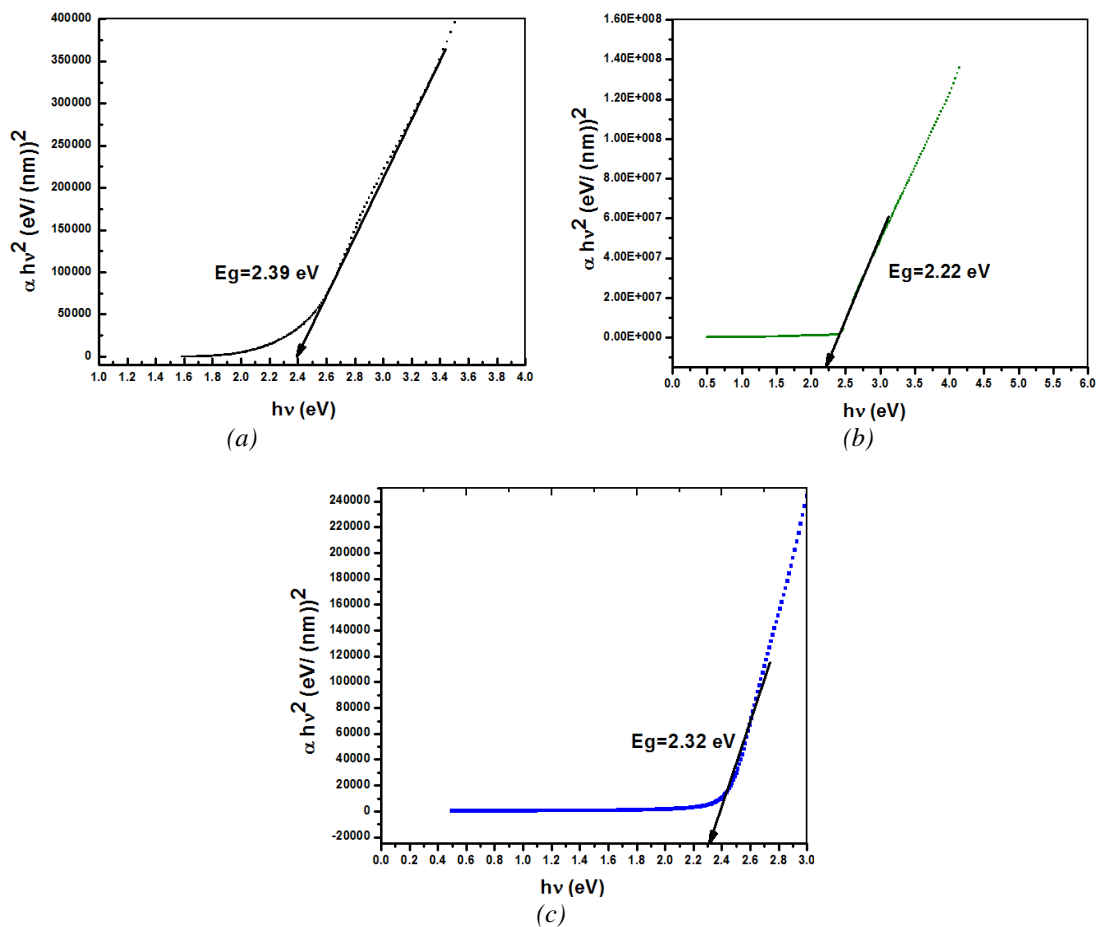


Fig. 4. Calculated band gap of: a) as prepared CdS nano powder, b) CdS prepared by spray pyrolysis technique, c) thermal evaporated CdS thin film.

As shown in Figure (4), the energy value (E_g) gradually varied by changing mechanism of preparation. The obtained values of CdS samples with found to be 2.3eV.

Figure 5 illustrate the spectral distribution of transmittance (T) and reflectance (R) of the as-prepared CdS thin films as a function of wavelength. The transmission spectra displayed a sharp absorption edge, indicating that CdS thin films could serve as effective optical filter materials. Notably, Figure (5) shows cased a distinct minimum in R at a wavelength falling within the 0.78-0.86 μm range, which corresponded to the maximum transmission for the films. It is observed that , interference fringes become less pronounced and eventually disappear as the thickness of the thin film increases beyond a certain limit. This is because the optical path difference between the interfering light waves becomes too large to produce noticeable interference effects.

The visibility and spacing of interference fringes are determined by the relationship between the wavelength of light and the film thickness. When the film thickness is on the order of the wavelength of light or smaller, the interference fringes are well-defined and easily observable. As the film thickness increases, the fringe spacing becomes wider, and the fringes may start to overlap or blur together.

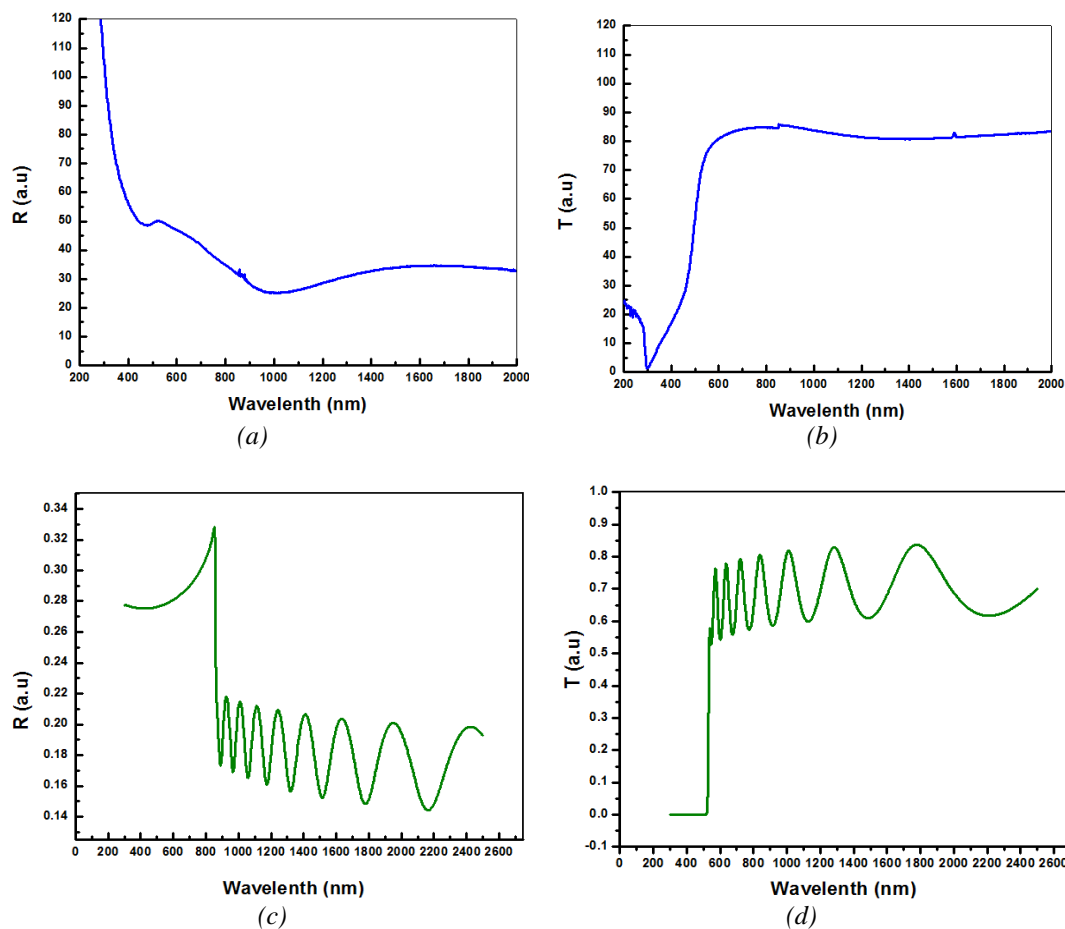


Fig. 5. Transmittance and Refraction of: a, b) CdS prepared by spray pyrolysis technique, c, d) thermal evaporated CdS thin film.

4. Conclusion

CdS thin films were successfully prepared by thermal evaporation and spray pyrolysis method from prepared CdS nanoparticles. The impact of varying preparation technique on the structure and optical properties was investigated. The hexagonal wurtzite structure of the CdS films was confirmed by XRD. In contrast, the CdS thin films prepared using the spray pyrolysis technique exhibited a polycrystalline nature. This disparity can be attributed to the greater porosity of the spray-deposited films. The low optical band gap energy exhibited by the CdS samples makes them promising candidates for potential applications in solar cells. The optical parameter of CdS thermal evaporated films suggested be calculated using Swanepoel method due to thinness of this films comparison to spray pyrolysis films.

Acknowledgments

The authors extend their appreciation to the Deanship of Scientific Research at King Khalid University, Saudi Arabia for funding this work through Large Groups Project under grant number R.G.P2/586/44.

References

- [1] R. Bhattacharya, S. Saha, *Journal of Physics*, 71, 187 (2008); <https://doi.org/10.1007/s12043-008-0152-7>
- [2] A. Dumbrava, C. Badea, G. Prodan, V. Ciupina, *Chalcogenide Letters*, 7, 111 (2010).
- [3] J. Travas-Sejdic, H. Peng, R. Cooney, G. Bowmaker, M. Cannell, C. Soeller, *Current Applied Physics*, 6, 562 (2006); <https://doi.org/10.1016/j.cap.2005.11.061>
- [4] T. Elango, S. Subermanian, K.R. Maurli, *Surf. Coat. Technol.*, 123(1), 8 (2003).
- [5] K. Sharma, A.S. Al-Kabbi, G.S.S. Saini, S.K. Tripathi, *Current Applied Physics*, 13, 964 (2013); <https://doi.org/10.1016/j.cap.2013.01.037>
- [6] V. Swaminathan, V. Subramanian, K.R. Murali, *Thin Solid Films*, 359, 113 (2000); [https://doi.org/10.1016/S0040-6090\(99\)00692-6](https://doi.org/10.1016/S0040-6090(99)00692-6)
- [7] R. Banerjee, R. Jayakrishnan, P. Ayyub, *J. Phys., Condens. Matter*, 12, 10647 (2000); <https://doi.org/10.1088/0953-8984/12/50/325>
- [8] Al. L. Efros, M. Rosen, *Annu. Rev. Mater. Sci.*, 30, 475 (2000); <https://doi.org/10.1146/annurev.matsci.30.1.475>
- [9] S. Rahman, K. Nadeem, M.A. Rehman, M. Mumtaz, S. Naeem, I.L. Papst, *Ceram. Int.*, 39, 5235 (2013); <https://doi.org/10.1016/j.ceramint.2012.12.023>
- [10] S.A. Wolf, et al., *Science*, 294(5546), 1488 (2001); <https://doi.org/10.1126/science.1065389>
- [11] E.D.T. Atkins, *Comprehensive Polymer Science and Supplements*, 1, 613-650 (1989); <https://doi.org/10.1016/B978-0-08-096701-1.00028-8>